Available online at www.sciencedirect.com

ScienceDirect

Energy Procedia 38 (2013) 368 – 374

Energy Procedia

SiliconPV: March 25-27, 2013, Hamelin, Germany

Influence of solder pads to PERC solar cells for module integration

Fabian Kiefer[a], Till Brendemühl[a], Miriam Berger[a], Anja Lohse[a], Sabine Kirstein[a], Nadja Braun[a], Martin Lehr[a], Frank Heinemeyer[a], Verena Jung[a], Arnaud Morlier[a], Susanne Blankemeyer[a], Iris Kunze[a], Renate Winter[a], Nils-Peter Harder[a,b], Thorsten Dullweber[a], Marc Köntges[a], Rolf Brendel[a,c]

[a] *Institute a Institute for Solar Energy Research Hamelin (ISFH), Am Ohrberg 1, D-31860 Emmerthal, Germany*
[b] *Institute of Eletronic Materials and Devices, Leibniz Universität Hannover, Schneiderberg 32, D-30167 Hannover, Gemany*
[c] *Institute for Solid State Physics, Leibniz Universität Hannover, Appelstr. 2, D-30167 Hannover, Germany*

Abstract

The majority of screen printed solar cells has silver pads at the rear side to enable soldering for the module manufacturing. The pads increase the recombination at the silicon/metal interface due to the absence of a back surface field (BSF) at the solder pads. This reduces the efficiency of full-area Al-BSF solar cells. For passivated emitter and rear cells (PERC), a large area fraction of the rear side is covered with the passivation layer. When using specially designed Ag pastes for the rear side of PERC cells, the passivation of this layer is maintained, and the rear recombination is reduced.

A comparison of solar cells with and without solder pads confirms that there is no loss in solar cell performance, both cell types achieve an efficiency of 19.6%. We investigate the influence of solder pads to PERC solar cells by calculating the effective rear surface recombination. The calculations confirm that there is a loss in open circuit voltage of less than 2 mV due to the solder pads.

A 54-cell PERC PV module is manufactured. The cell-to-module loss reveals that the module process is still to be optimized. Comparable modules made from 9 solar cells lost less than 1% relative in all *J-V* parameters after a 1000 h damp-heat test.

Keywords: Solar Cells, PERC, Solder Pads, Metallisation, PERC PV module

doi:10.1016/j.egypro.2013.07.291

1. Introduction

Today, many solar cell manufacturers take efforts to introduce PERC solar cells into production. Recently, the development of screen-printed PERC solar cells led to efficiencies of more than 20% with a peak efficiency of 21% [1,2,3]. But there is also the need to integrate these higher efficient PERC solar cells into PV modules. The majority of screen-printed solar cells feature Ag solder pads on the rear side because the aluminum on the rear side is not solderable to the cell interconnect ribbons. One alternative is the industrially available thin pad technique which enables solder pads direct on the aluminum paste of the solar cells [4].

The Ag solder pads are known to reduce the efficiency of full-area back surface field (BSF) solar cells by 0.2% absolute [5] due to the high recombination at the silicon-metal interface. In PERC solar cells, the solder pad has less effect to the cell efficiency due to the passivation layer between solder pad and silicon bulk layer, if the Ag pad paste does not fire through the rear passivation layer during the firing process. The Ag/Si interface area is therefore significantly reduced. We investigated the impact of the solder pads on the PERC solar cell performance. We build a demonstrator module of our PERC solar cells to demonstrate the functionality of the pads.

2. Experimental

Baseline front end process

A baseline reference process was established at ISFH for screen-printed PERC solar cells. We reached efficiencies of 20.1 % with this reference process [2]. The solar cell process flow is schematically shown in Figure 1. Most of the process steps are carried out on industrially feasible machines in ISFH SolarTec. We use boron doped 15.6 cm x 15.6 cm pseudosquare Czochralski grown silicon wafers with an area of 233.4 cm² and a bulk resistivity of 2-3 Ωcm. After wafer cleaning and KOH damage etch, a rear side protection layer is deposited to protect the rear side during texture etch. The layer also protects the rear side in the subsequent phosphorous diffusion process. Subsequently, the protection layer is removed during the PSG removal.

Alternative front end process

Further solar cells that we use for solder and module tests are manufactured using a novel process with double-sided texture and phosphorous diffusion. A single-side polish process etches the P diffusion from the rear side. A detailed description of this process and a schematic of the process flow is given by C. Kranz [6]. This process shows efficiencies that are equal to the reference process. Those cells have a non-planar rear side in comparison to solar cells examined so far. In fact, most processes for module integration have to be re-evaluated for single-side polished cells since the rear side is not fully planar after polishing.

Back end cell process

Subsequently, passivation layers are deposited on front and rear side. On the rear side, we use an atomic layer deposited (ALD) Al_2O_3 passivation layer which is capped by a silicon nitride (SiN_x), grown by plasma-enhanced chemical vapor deposition (PECVD). The front side is passivated with a PECVD-grown SiN_x layer with a refractive index of 2.05. After passivation, we prepare line-shaped laser contact openings (LCO) by ablation. The pulses have a duration of 9 ps and a wavelength of 532 nm. In the next steps, the front and rear side metallization are screen-printed on the wafer with Al and Ag pastes. For the solder pads, we use a silver paste designed for PERC solar cells in order not to fire through the rear passivation layer. All pastes are commercially available.

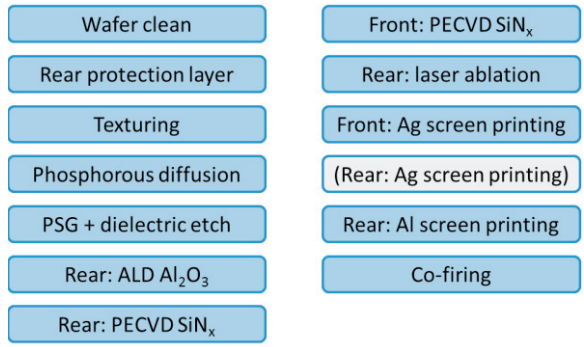

Fig. 1. Process flow of the PERC solar cells with optional printing of the solder pads on the rear side

The pastes are dried in a belt furnace at 200°C after each printing step and the cells are co-fired in a conveyor belt furnace at a peak temperature of 840°C. We printed two batches of cells: One with Ag solder pads on the rear side and one without solder pads. This permits the quantification of the impact of the solder pads on the cell performance.

Module process

The solar cells are tabbed using a solar cell stringer from IMA. All solder experiments are conducted using automated soldering with the solar cell stringer. We use copper interconnector ribbons from Schlenk with a $Sn_{62}Pb_{36}Ag_2$ solder layer and with dimensions of 0.15 mm x 2 mm and Kester 952S flux agent. The hot plate at the solder spot in the stringer is kept at a temperature of 165°C and the soldering irons are set to 230-235°C. A 180° peeling test measures the force necessary to peel the ribbon from the solar cell. After peeling off the interconnector ribbons, we determine the fracture mode with a microscope. To assure a bubble free lamination of the PV modules and the subsequent damp-heat test, the cells are dipped into 70°C warm deionized water for 10 min. There should be no gas effusion from the pastes, which would result in small bubbles on the cell surface. All cells have been light degraded and measured separately after the light-induced degradation (LID). The strings used for the modules are soldered in the IMA stringer. String interconnection and lamination are conducted manually.

One 54-cell module and three 9-cell modules are manufactured. The 9-cell modules are accelerated aged in a damp-heat test as instructed in the standard IEC 61215 [7].

3. Influence of solder pads on solar cell level

In the following, we compare a group of 6 screen-printed PERC solar cells with solder pads and 5 cells without solder pads. The solar cells have continuous line contacts on the rear side and underneath the solder pads. The in-house-measured light *J-V* parameters and the J_{01} values of the groups are summarized in Table 1. The J_{01} of our cells have been fitted from J_{SC}-V_{OC} measurements of our PERC solar cells. In both solar cell groups, the variations of V_{OC}, J_{SC}, FF and η are smaller than $1\%_{rel}$. The observed variance in open circuit voltage (V_{OC}) within one group is larger than the difference between the mean values of the two groups, which accounts to 1.1 mV. Therefore the impact of the solder pads on our screen-printed PERC solar cells is below detection limit of our experiment.

Table 1. IV parameters of groups of 6 solar cells without and 5 with solder pads on the rear side including the deviations between maximum and minimum value.

Cell type	V_{oc} (mV)	J_{sc} (mA/cm^2)	FF (%)	η (%)	J_{01} (fA/cm²)
Without solder pads	645.3 ± 1.4	38.14 ± 0.15	78.9 ± 0.7	19.42 ± 0.10	375 ± 24
With solder pads	646.4 ± 1.7	38.20 ± 0.12	78.4 ± 0.5	19.36 ± 0.17	370 ± 29

4. Calculations of rear recombination

In order to understand the observed absence of any significant V_{OC} loss due to solder pads, we calculate the effective rear recombination for PERC solder cells. Figure 2 sketches the cross-section of a PERC cell. The Ag solder pads (dark grey in Fig. 2) have a detrimental influence on the solar cell performance due to the absence of a back surface field (green in Fig. 2) underneath the pads [5]. However, more than 90% of the rear side is passivated for PERC solar cells (light blue in Fig. 2). Consequently, the area fraction of the Ag/Si interface at the solder pad, i.e. the Ag-metallized silicon surface without a BSF, is also reduced from 4.6% to 0.32% (whole pad region compared to blue/dark grey contact region in Fig. 2).

To quantify the impact of the pad region, we calculate the 1D equivalent surface recombination velocity (SRV) $S_{rear,1D}$ for the solder pad region and the BSF region. We use the formulas published by Plagwitz [8] and Fischer [9] to calculate $S_{rear,1D}$ values for local contacts. As depicted in figure 2, we conceptually divide the solar cell into two regions: The pad region is the area taken in by the sum of all solder pads, and the BSF region is the sum of all regions with Al-BSF at the contact openings. The total solar cell is calculated from both regions operating in parallel as shown in figure 2, i.e. the equivalent 1-dimensional $S_{rear,1D}$ value of the total cell rear side is the area weighted $S_{rear,1D}$ values of the two regions. The surface recombination at the ALD-Al_2O_3 passivated rear surface is assumed to be S_{pass} = 7.5 cm/s [2] and the S-value of the BSF is S_{BSF} = 350 cm/s [10]. The surface recombination at the Ag/Si interface is assumed to be the thermal velocity $S_{Ag} = 1 \cdot 10^7$ cm/s. We calculate the SRV values for line contacts in the BSF region and for a 160 µm thick wafer with a bulk doping of 2 Ωcm.

For comparison we also calculate the $S_{rear,1D}$ of the pad region with point contacts instead of line contacts in the pad region. We assume points with the same pitch as between the contact lines. We use a point diameter which leads to the same area fraction for the openings as for the line contacts. This point contact value for the $S_{rear,1D}$ of the pad region is lower than that of a pad region with line contacts.

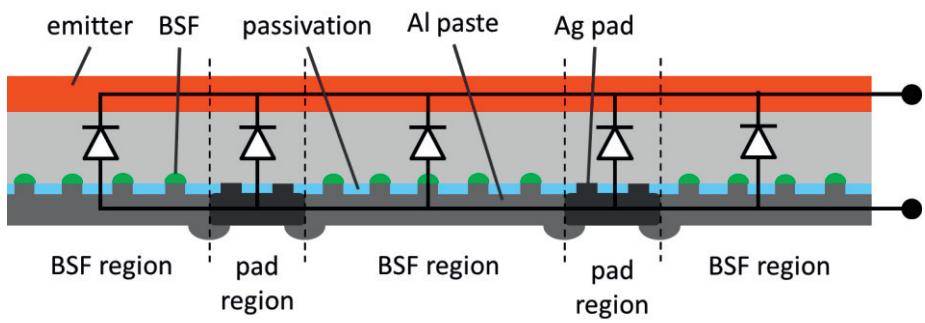

Fig. 2. Schematic concept of the solar cell which is divided into a BSF region and a solder pad region connected in parallel.

Thus, we regard the $S_{rear,1D}$ for line contacts as an estimation for the maximum recombination enhancement due to the Ag/Si interface at the solder pads. Possible interactions at the edge between Ag and Al metallization are neglected.
The calculated surface recombination velocity for the 1D equivalent $S_{rear,1D}$ at the solder pad and the BSF region, the resulting SRV and the rear recombination current $J_{0,rear}$ for the entire rear side are listed in Table 2. For the calculation, a cover fraction of 4.6% for the solder pads is assumed. The calculations show, that the maximum enhancement of rear recombination accounts for 15 cm/s due to the Ag/Si interface without back surface field.

This corresponds to an increase of 31 fA/cm² in recombination current density. A screen printed solar cell typically has a recombination current density higher than 300 fA/cm², as can be seen also on the cells in table 1. This corresponds to a recombination enhancement of about 10%, resulting in an open circuit voltage reduction of less than 2 mV.

Table 2. Calculated $S_{eff,rear}$ and $J_{0,rear}$ parameters for a rear side with and without solder pads (SPad) assuming line or point contacts with an opening area fraction of 6.6%.

Cell type	$S_{rear,1D}$ in Pad region (cm/s)	$S_{rear,1D}$ in BSF region (cm/s)	$S_{rear,1D}$ entire rear side (cm/s)	$J_{0,rear}$ entire rear side (fA/cm^2)
Without solder pads		30	30	62
With solder pads (lines)	350	30	45	93
With solder pads (points)	210	30	38	79

5. Module manufacturing

Further investigations concentrate on the module integration of the PERC solar cells from the single-side polish process [6]. As mentioned before, those cells have a non-planar rear side. Thus, most processes for module integration have to be re-evaluated for those cells. Figure 3 shows the results of the 180° peeling test for the three interconnector ribbons of exemplary cells. Due to the automatic contact soldering and partionated solder pads on the cell rear side the peel force drops down in-between the solder iron imprints on the front side and between the solder pad on the rear side.

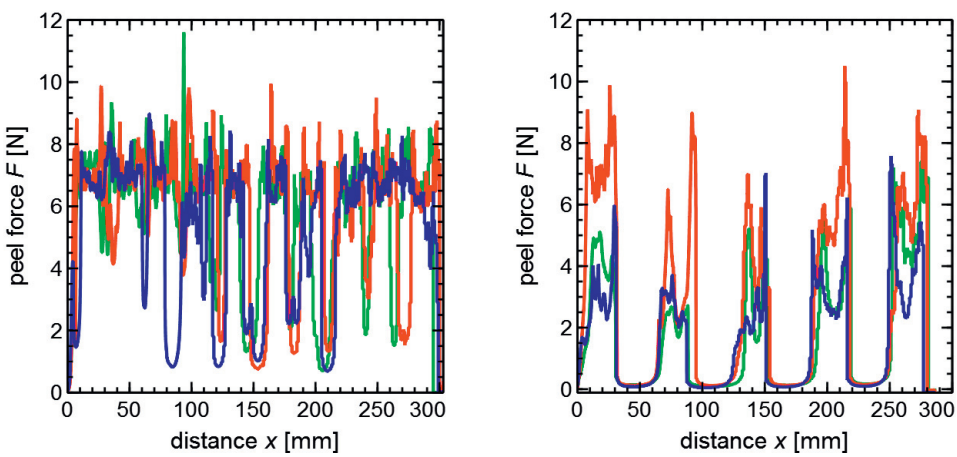

Fig. 3. Peel forces for the 3 tabs (red, green and blue) of exemplary solar cells:
front side (left) and rear side (right) with 5 separate solder pads

The peel forces on both cell sides are higher than 1 N per interconnector ribbon (as required in [11]). They show a maximum peel force of more than 8 N. The fracture mode is an adhesion fracture in the solder or in the silver paste. The PERC solar cells also passed the gas effusion test, as described above.

We build a 54 cell module. The PERC module has a maximum power of 224.1 W under standard test conditions. The sum of maximum powers of the non-encapsulated 54 cells is 240.3 W after light induced degradation. The cell-to-module power loss according to Ref. [12] is thus 7%. We detected an enlarged series resistance, which reduces the fill factor of the module to 74.8%. The mean value of the used PERC solar cells was 78.2%. We explain the enlarged series resistance with a partial peeling of the interconnector tabbings from the rear side due to the bow of the solar cells. A linear extrapolation to a 60 cell module yields an extrapolated power of 249 W. The module process is not yet optimized. The wafers used for the PV module have a smaller diameter of 190 mm at the wafer edges compared to most wafers available nowadays. Wafers with a greater, typical diameter (200 mm) have a 2.4% larger active cell area. The antireflection coatings on the solar cells have not yet been optimized for integration of the cells into modules.

We also build three smaller modules with 9 cells from the same cell batch. After a 1000h damp-heat test (according to [7]), the three modules show a loss of 0.1 – 0.8%$_{rel}$ in peak power. All important *J-V* parameters are above 99.2% of the initial values (see Table 3). The main power loss is caused by a loss in J_{SC}. We assume a transparency loss of the EVA during the test.

Table 3. Relative values of important *J-V* parameters for three 9-cell test modules after 1000h damp-heat.

Module No.	V_{OC} (%$_{rel}$)	J_{SC} (%$_{rel}$)	*FF* (%$_{rel}$)	P_{mpp} (%$_{rel}$)
1	100.0	99.5	100.5	99.9
2	99.7	99.5	100.0	99.2
3	99.9	99.9	100.0	99.7

6. Summary

We investigated the impact of silver solder pads on the performance of screen-printed PERC solar cell. Experimentally we could find no influence of the solder pads within measurement accuracy. Theoretical estimations of the effective SRV values of the rear sides show that the pads of PERC cells increase the effective SRV from 30 cm/s to 45 cm/s. There is thus a maximum increase of 15 cm/s due to the Ag/Si contact. The calculated SRV enhancement should cause a maximum loss of 2 mV in open circuit voltage for screen-printed solar cells, resulting in a difference of 0.06%$_{abs}$ in efficiency. There is thus no significant influence on the efficiency of the PERC solar cell, in contrast to full-area BSF solar cells, which suffer from a loss of 0.2%$_{abs}$ in efficiency.

PERC Solar cells made with a novel single-side polish process were manufactured and successfully brought into a 54-cell solar module. The peel force and the fracture mode have been tested on the PERC solar cells before manufacturing the module. Modules with 9 PERC cells have successfully performed a damp-heat test with a degradation of less than 0.8% in 1000 h.

Acknowledgements

We thank all our colleagues at ISFH for the support at all steps of the PERC solar cell process and at module manufacturing. We also acknowledge Heraeus Precious Materials for the pad silver paste supply.

References

[1] P. Engelhart, et. al., “Q.antum – Q-Cells Next Generation High-Power Silicon Cell & Module Concept”, Proceedings of the 26th European Photovoltaic Solar Energy Conference, Hamburg, Germany, 2011, pp. 821-826

[2] T. Dullweber, C. Kranz, B. Beier, B. Veith, J. Schmidt, B.F.P. Roos, O. Hohn, T. Dippell, R. Brendel, “Inductively coupled plasma chemical vapour deposited AlOx/SiNy layer stacks for applications in high-efficiency industrial-type silicon solar cells”, Solar Energy Materials & Solar Cells 112, pp. 196–201 (2013)

[3] K. Ramspeck, et. al., “Light-Induced Degradation of Rear Passivated mc-Si Solar Cells”, Proceedings of the 27th European Photovoltaic Solar Energy Conference, Frankfurt/Main, Germany, 2012, pp. 861-865

[4] H. v. Campe, S. Huber, S. Meyer, S. Reiff, J. Vietor, “Direct Tin-Coating of the Aluminum Rear Contact by Ultrasonic Soldering”, Proceedings of the 27th European Photovoltaic Solar Energy Conference, Frankfurt/Main, Germany, 2012, pp. 1150-1153

[5] Schmid group “SCHMID's Silver-Free Backside affords great Cost Reductions for Mass Production”, Press release

[6] C. Kranz, et. al., “Wet chemical polishing for industrial type PERC solar cells”, this conference

[7] Standard IEC 61215

[8] H. Plagwitz, R. Brendel, “Analytical model for the diode saturation current of point-contacted solar cells” Progress in Photovoltaics, 14 (1), pp. 1-12 (2006)

[9] B. Fischer, “Loss Analysis of Crystalline Silicon Solar Cells using Photoconductance and Quantum Efficiency Measurements”, Ph.D. thesis, University of Konstanz, Germany, 2003

[10] T. Dullweber, et. al., “20.1%-Efficient Industrial.Type PERC Solar Cells Applying ICP AlOx as Rear Passivation Layer”, Photovoltaics International 17, 72 (2012)

[11] Standard DIN EN 50461

[12] M.A. Green, Solar Cells-Operating Principles, Technology and System Applications, Prentice Hall Inc. Englewood Cliffs, 1982, pp. 161-164